AGU PUBLICATIONS

Space Weather

RESEARCH ARTICLE
10.1002/2016SW001425

Key Points:
- We demonstrate an improved model of the Earth's radiation environment and compare it to airline and balloon based measurements
- We find the model to be sufficiently accurate to assess radiation risks in Earth's atmosphere
- This model will be made available to the community for future efforts in risk assessment and the study of atmospheric radiation

Correspondence to:
C. J. Joyce,
cjl46@wildcats.unh.edu

Citation:
Joyce, C. J., et al. (2016), Atmospheric radiation modeling of galactic cosmic rays using LRO/CRaTER and the EMMREM model with comparisons to balloon and airline based measurements, *Space Weather*, *14*, 659–667, doi:10.1002/2016SW001425.

Received 18 MAY 2016
Accepted 11 AUG 2016
Accepted article online 18 AUG 2016
Published online 10 SEP 2016

Atmospheric radiation modeling of galactic cosmic rays using LRO/CRaTER and the EMMREM model with comparisons to balloon and airline based measurements

C. J. Joyce[1], N. A. Schwadron[1], L. W. Townsend[2], W. C. deWet[2], J. K. Wilson[1], H. E. Spence[1], W. K. Tobiska[3], K. Shelton-Mur[4], A. Yarborough[5], J. Harvey[5], A. Herbst[5], A. Koske-Phillips[5], F. Molina[5], S. Omondi[5], C. Reid[5], D. Reid[5], J. Shultz[5], B. Stephenson[5], M. McDevitt[5], and T. Phillips[6]

[1]Physics Department, Space Science Center, University of New Hampshire, Durham, New Hampshire, USA, [2]Department of Nuclear Engineering, University of Tennessee, Knoxville, Knoxville, Tennessee, USA, [3]Space Environment Technologies, Pacific Palisades, Los Angeles, California, USA, [4]FAA Office of Commercial Space Transportation, Washington, District of Columbia, USA, [5]Earth to Sky Calculus, [6]Spaceweather.com

Abstract We provide an analysis of the galactic cosmic ray radiation environment of Earth's atmosphere using measurements from the Cosmic Ray Telescope for the Effects of Radiation (CRaTER) aboard the Lunar Reconnaissance Orbiter (LRO) together with the Badhwar-O'Neil model and dose lookup tables generated by the Earth-Moon-Mars Radiation Environment Module (EMMREM). This study demonstrates an updated atmospheric radiation model that uses new dose tables to improve the accuracy of the modeled dose rates. Additionally, a method for computing geomagnetic cutoffs is incorporated into the model in order to account for location-dependent effects of the magnetosphere. Newly available measurements of atmospheric dose rates from instruments aboard commercial aircraft and high-altitude balloons enable us to evaluate the accuracy of the model in computing atmospheric dose rates. When compared to the available observations, the model seems to be reasonably accurate in modeling atmospheric radiation levels, overestimating airline dose rates by an average of 20%, which falls within the uncertainty limit recommended by the International Commission on Radiation Units and Measurements (ICRU). Additionally, measurements made aboard high-altitude balloons during simultaneous launches from New Hampshire and California provide an additional comparison to the model. We also find that the newly incorporated geomagnetic cutoff method enables the model to represent radiation variability as a function of location with sufficient accuracy.

1. Introduction

Recent projections of the interplanetary radiation environment performed by *Schwadron et al.* [2014] indicate that the current trend of declining solar activity will lead to elevated galactic cosmic ray (GCR) fluxes and increasingly hazardous conditions for spacecraft crew members. As a result of their analysis, *Schwadron et al.* [2014] proposed that it may be preferable to schedule exploration missions during solar maximum, when increased solar activity and stronger heliospheric magnetic fields reduce the flux of GCRs. This would represent a significant shift in the strategic planning of exploration missions, where previously solar minimum would have been considered preferable due to the decreased frequency of extreme solar energetic particle events. Advancements in the prediction capabilities for the arrival of interplanetary coronal mass ejections combined with the relative effectiveness of spacecraft shielding on solar energetic particle (SEP) radiation serve to make solar storms less dangerous to spacecraft crew members than they were previously thought to be. For example, *Joyce et al.* [2015] used radiation modeling of the 23 July 2012 event observed by STEREO A, an extreme space weather event that initially drew many comparisons to the historic Carrington Event, to show that with the benefit of heavy protective shielding (10 g/cm^2 aluminum), astronauts aboard a spacecraft would be exposed to levels of radiation well below NASA's permissible exposure limits [*NASA*, 2007]. On the other hand, due to their relatively high energy and nearly constant flux, GCRs represent a persistent radiation threat for which increased shielding is not as effective since the secondaries produced by the penetrating particles within the shielding can often be more damaging than the GCRs themselves. It is clear that given recent findings, accurate radiation modeling of GCRs is essential for the planning of future manned

exploration missions. Atmospheric radiation modeling may gain increased significance given the recent announcement that NASA will be working to develop supersonic passenger transports that will fly at altitudes much higher than normal commercial aircraft, thus reducing the level of atmospheric shielding and increasing the radiation risk. Additionally, atmospheric shielding of radiation is an important consideration for potential manned missions to Mars.

In this study, we provide an analysis of the radiation impact of GCRs in Earth's atmosphere using measurements made by the Cosmic Ray Telescope for the Effects of Radiation (CRaTER) [*Spence et al.*, 2010], an instrument aboard the Lunar Reconnaissance Orbiter (LRO) [*Chin et al.*, 2007] designed to measure energetic particles above 10 MeV, together with the Badhwar-O'Neil model described by *O'Neill* [2006] and dose lookup tables computed by the high charge and energy transport computer program (HZETRN) [*Nealy et al.*, 2007] and the high-energy transport code (HETC-HEDS) [*Townsend et al.*, 2005], which are components of the Earth-Moon-Mars Radiation Environment Module (EMMREM) [*Schwadron et al.*, 2010]. This work is based on the modeling performed by *Joyce et al.* [2014], using updated lookup tables to improve the accuracy of the analysis. While *Joyce et al.* [2014] computed dose rates only for the polar regions, where the open field lines of Earth's magnetosphere have little effect on radiation levels, this study applies the geomagnetic cutoff calculation method of *Nymmik et al.* [2009] to account for the effect of the Earth's magnetosphere on penetrating GCRs and the resulting atmospheric radiation levels, enabling the model to compute dose rates at different geographic positions as a function of latitude and longitude. Newly available measurements of GCR radiation made by instruments aboard commercial airlines as well as high-altitude balloons afford the opportunity to test the accuracy of the model in computing dose rates in the Earth's atmosphere. Validation of the model via direct observations lends credibility to the model and paves the way for its use in future risk assessment efforts and radiation studies.

2. Overview of Model and Measurements

Previously, *Joyce et al.* [2013] described a method for using GCR dose rates together with EMMREM-generated dose lookup tables to compute the modulation potential, i.e., the amount of energy lost by GCRs as they stream through the heliosphere due to interaction with the interplanetary magnetic field. Using a single modulation potential to represent the energy lost by GCRs regardless of ion species or energy is a common simplifying assumption that yields sufficiently accurate results. Using an archive of CRaTER radiation measurements (the D1-D2 dose rate described in detail by *Schwadron et al.* [2012]) taken during quiet times when GCRs dominate the observed radiation together with dose lookup tables generated by the HZETRN code [*Townsend et al.*, 2011] and the GCR transport model of *O'Neill* [2006], *Joyce et al.* [2013] showed the evolution of the modulation potential over the course of the LRO mission to that point, from the bottom of the protracted solar minimum of solar cycle 23 and into the ascending phase of cycle 24. Figure 1 shows an updated version of the plot that originally appeared in *Joyce et al.* [2013] showing the modulation potential, galactic cosmic ray dose rate, and the mean daily sunspot number over the course of the LRO mission to date. In a subsequent study, *Joyce et al.* [2014] used this computed modulation potential together with similar lookup tables to compute atmospheric dose rates at Earth and Mars. Following the publication of *Joyce et al.* [2014], it was discovered that an error had been made in the calculations using the HETC-HEDS code to generate the Earth atmosphere dose lookup tables, resulting in underestimated radiation levels. The dose rates computed for the atmosphere of Mars in *Joyce et al.* [2014] were computed using a separate set of tables generated by the HZETRN code and were unaffected by this error. The error has since been corrected and the tables regenerated for use in this study.

We follow the same basic approach as *Joyce et al.* [2014] using the newly generated lookup tables to compute dose rates in Earth's atmosphere for various altitudes. We use the modulation potential shown in Figure 1 as input to a program that uses the Badhwar-O'Neill model described by *O'Neill* [2006] (based on the original formalism laid out by *Badhwar and O'Neill* [1992]) which solves for the transport of the interstellar GCR spectra to the Earth. Previously, *Joyce et al.* [2014] had ignored the effect of the magnetosphere on energetic particles entering Earth's atmosphere, computing dose rates only for the polar regions where open field lines have little effect on penetrating GCRs. For this study, we have incorporated the geomagnetic cutoff model of *Nymmik et al.* [2009] in order to take into account the shielding provided by the Earth's magnetic field, thus enabling the model to produce dose rates for any latitudinal or longitudinal position in the Earth's atmosphere. The geomagnetic cutoff model shown by *Nymmik et al.* [2009] was chosen for use in the study because of its simplicity and ability to accurately calculate geomagnetic cutoffs with little computational power required.

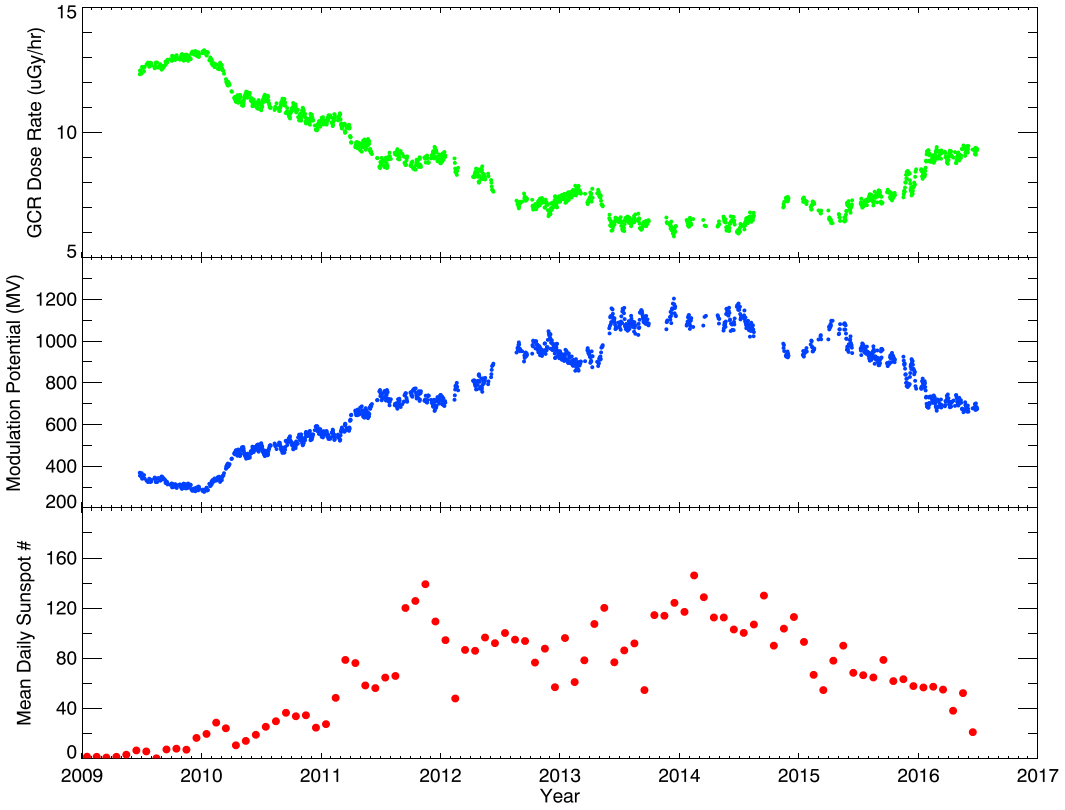

Figure 1. Plot of the (middle) modulation potential over the course of the LRO mission. Also shown is the (top) GCR dose rate measured by CRaTER and the (bottom) average daily sunspot number provided by the Solar Influences Data Analysis Center, which shows the evolution of the solar cycle. This is an updated version of the original plot shown in *Joyce et al.* [2013].

Using the *Kp* index (available at: http://www.ngdc.noaa.gov/) as input to account for the effect of solar activity on the Earth's magnetosphere, this method computes a vertical cutoff rigidity (generally considered a sufficient approximation for the cutoff rigidity averaged over all directions *Nymmik et al.* [2009]) for a given latitudinal and longitudinal position. Using the computed rigidity, we then compute radiation levels using only particles with magnetic rigidities greater than the geomagnetic cutoff. Using this modified flux spectrum together with dose tables generated by the HETC-HEDS code, we are able to compute dose rates for any geographic position at various altitudes in the Earth's atmosphere, extending down to commercial airline altitudes (11 km). The particles accounted for in the computation of these dose rate tables include protons, heavy ions from He to Fe, and secondary neutrons, pions, and muons, with all particle energy losses being deposited locally at the site of the collision. Π_0 particles were not transported in this calculation, with all their energy being deposited locally at the site of their production.

The Automated Radiation Measurements for Aerospace Safety (ARMAS) project has recently made available a data set of radiation measurements made aboard commercial and research aircraft flights spanning from 2013 to 2016, enabling the first validation of this atmospheric radiation model via direct measurement. The ARMAS project uses dosimeter sensors aboard aircraft in order to provide radiation data for efforts in Earth science research and to improve aviation safety. The data used in this study are available at: http://sol.spacenvironment.net/~ARMAS/Level_2_3_Data.html. The dosimeters used in the ARMAS project measure the total ionizing dose resulting from protons, heavy ions, and neutrons in addition to gamma rays, which is comparable to the species that are used in the model.

A newly available and expanding data set of atmospheric radiation measurements made by instruments aboard high-altitude balloons provide an additional source of atmospheric radiation data and comparison to the model. These balloon launches were undertaken as a part of the Earth to Sky Calculus program, in which high school students mentored by Dr. Tony Phillips of spaceweather.com conduct experiments to study the Earth's atmosphere using instruments launched on high-altitude balloons (for more information on this

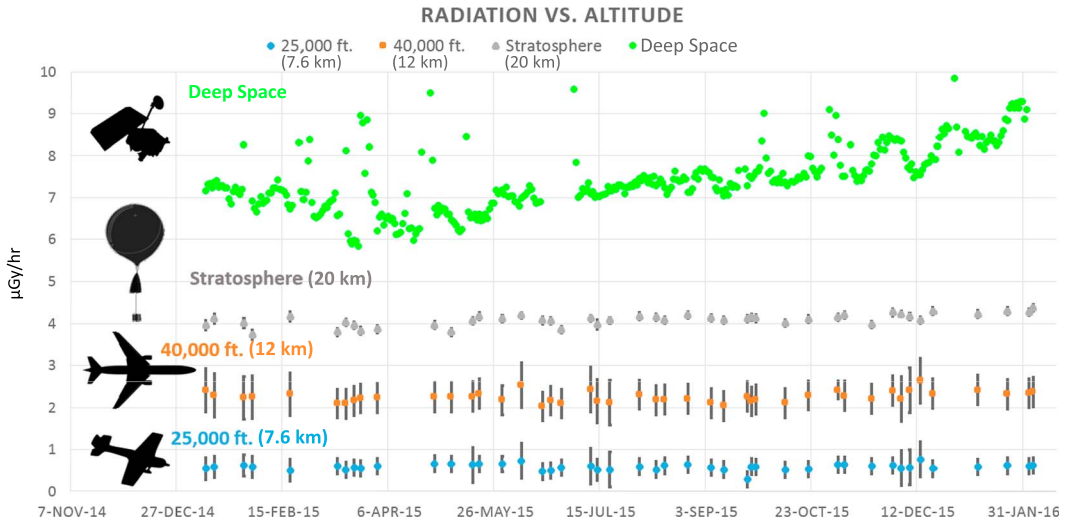

Figure 2. Radiation data from 25 high-altitude balloon launches made from California over the course of 2015 for three altitudes corresponding to the stratosphere and to common cruising altitudes of large commercial airliners and smaller propeller-driven planes. Each measurement is averaged over four separate dosimeters aboard the balloon. Dose rates for interplanetary space over this period are provided by CRaTER.

program, see: http://earthtosky.net/). The instrument used in these launches to measure dose rates is the Polimaster 1621M dosimeter, which measures radiation caused by the X-rays and gamma ray secondaries that are emitted as a result of the interaction of the penetrating GCRs with the Earth's atmosphere. Each payload typically includes four of these sensors, with the resulting measurements being an average of the four detectors. Because the balloon-based instruments measure radiation only from photons, while the model accounts for the radiation due to particles, these measurements do not provide a means of validation for the model but instead offer an opportunity to observe how the radiation due to photons and particles compare as a function of altitude in Earth's atmosphere. The data set contains two examples of measurements taken during simultaneous launches from Bishop, California (lat: 37.5°, long: −118.9°), and Concord, New Hampshire (lat: 43.2°, long: −71.5°), providing an opportunity to compare how geographic location affects the atmospheric radiation profiles of photons and particles. In 2015, the students launched 42 balloons, including 40 from California and 2 from New Hampshire. Figure 2 shows atmospheric dose rates taken from this data set for three different altitudes, with CRaTER measurements providing the dose rate in space over this time period.

3. Results

Using the modulation potential shown in Figure 1, we compute atmospheric dose rates over the course of the LRO mission as shown in Figure 3. These atmospheric dose rates are computed for the same latitude and longitude as for the California balloon launches, in order to be comparable to the dose rates plotted in Figure 2. The dose rate in interplanetary space, as measured by CRaTER, is also included in the plot for reference. We see that due to the corrections made to the dose tables, these dose rates are significantly higher than those reported by *Joyce et al.* [2014] and also that there is less of a drop in the dose rates from high to low altitudes, with the dose rates at the highest altitude being close to those measured by CRaTER, particularly later in the LRO mission, and about a factor of 8 greater than those at the lowest altitude throughout. We also plot the dose rate for zero atmospheric shielding (labeled "High" in Figure 3) in order to demonstrate the pure effect of the magnetosphere on the radiation level. We see that the magnetic field alone reduces the dose rate by about 35% on average relative to the CRaTER dose rate and that the atmospheric shielding at 36 and 30 km (5 and 12 g/cm^2, respectively) actually serves to increase the dose rate, reducing the CRaTER dose rate by only 24%. This suggests the presence of a Pfotzer maximum in the radiation due to particles somewhere above 36 km, with the dose rate does not falling below the zero atmosphere levels until an altitude of approximately 25 km.

Figure 4 shows the comparison between the model and the level 3 ARMAS (version v5.35) dose rates measured on 117 airline flights spanning from 18 June 2013 to 18 February 2016. Dose rate, latitude, longitude, and altitude data for each flight were averaged and the average geomagnetic cutoff during the flight as computed

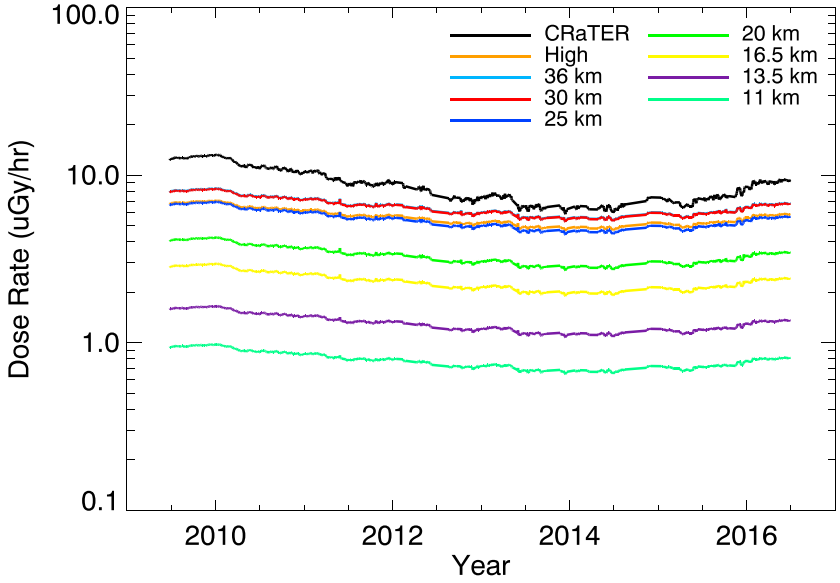

Figure 3. Plot of modeled GCR dose rates in the Earth's atmosphere over the course of the LRO mission to date. The model dose rates shown are computed using the Badhwar-O'Neil model together with the computed modulation potential shown in Figure 1 and updated EMMREM-generated dose lookup tables. Also shown for comparison is the CRaTER GCR dose rate measured over this period.

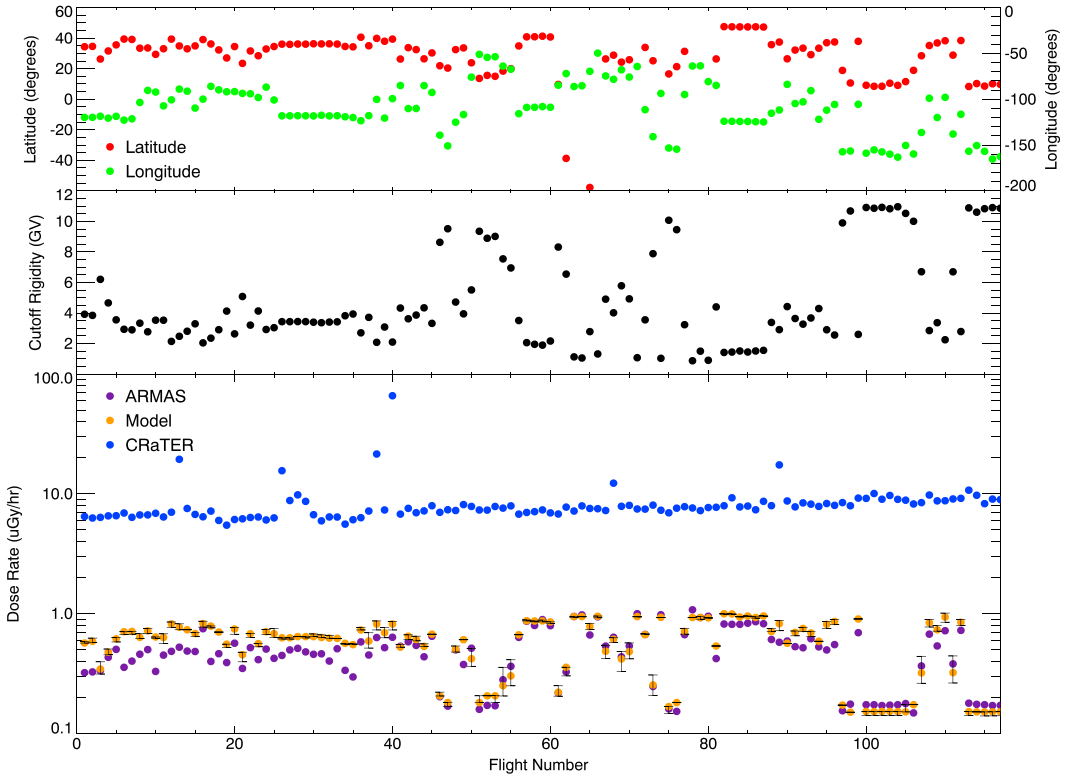

Figure 4. Dose rates measured aboard commercial aircraft during 117 flights spanning from mid-2013 to early 2016, as provided by the ARMAS project. Modeled dose rates are also shown and are found to be 20% greater than the measurements on average. The average latitude and longitude as well as the cutoff rigidity used by the model are plotted to explain how variations seen in the airline dose rates generally result from positional differences which determine the cutoff rigidity. Errors in the modeled dose rate are computed using the standard deviation of the geomagnetic cutoff for each flight, providing upper and lower limits on the dose rate. The dose rate measured by CRaTER during each flight is also shown for comparative purposes.

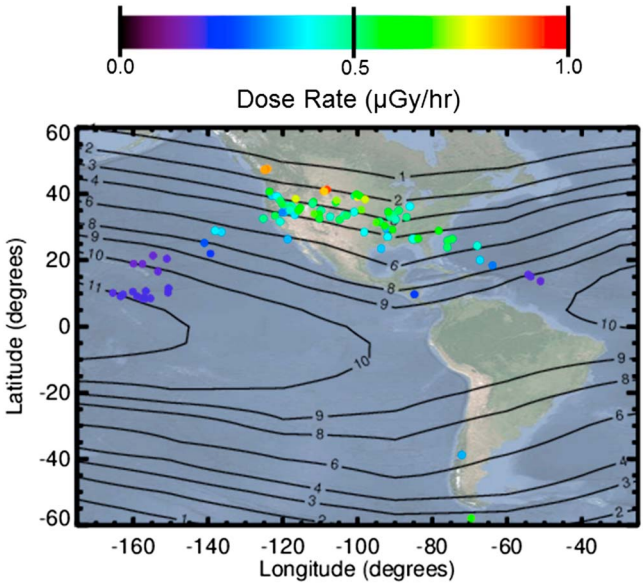

Figure 5. ARMAS dose rates as a function of latitude and longitude. The black lines are a contour plot of the geomagnetic cutoff rigidity (GV) using the cutoff rigidities computed by the model at an altitude of 11 km. The cutoff rigidities are computed using the average *Kp* index over the time span of the ARMAS measurements (1.8) and a local time of 12 P.M. for each location. We see that the variations in the measured dose are mostly ordered by location and the typical local cutoff rigidity, though time-dependent factors such as or geomagnetic activity and the GCR modulation are also responsible for some variation in the measured dose rates.

by the *Nymmik et al.* [2009] method was used as input for the atmospheric model to generate dose rates for comparison. In order to be comparable to the model's lowest altitude output (11 km), data measured below 8 km were not used for this comparison. Additionally, in order to have the geomagnetic cutoffs computed by the model be sufficiently accurate for this comparison, for each flight, data for latitudes and longitudes differing from the flight average by more than 5° and 15°, respectively, were discarded. The 117 flights used have been numbered in chronological order and plotted against the corresponding modeled dose rates in Figure 4. The ARMAS dose rate data are presented in terms of personal dose equivalent at a depth of 10 mm into tissue, generally considered a sufficiently precise assessment of the effective dose [*International Commission on Radiological Protection (ICRP)*, 2007] and is computed using quality factors that are estimated based on the cutoff rigidity. As shown by *Joyce et al.* [2014], the model does a poor job of computing dose equivalent rates using the operational quality factor derived from the linear energy transfer of the particles, and so for this comparison we divide the ARMAS dose equivalent rates by the average estimated quality factor to get the measured absorbed dose rate. Given the simplicity and limitations of the model, we see that the model does a fair job of reproducing the ARMAS measurements, with the model producing dose rates that are on average 20% higher than the measurements, which falls within the 30% uncertainty limit for radiation measurements recommended by the International Commission on Radiation Units and Measurements (ICRU) [*International Commission on Radiation Units and Measurements (ICRU)*, 2010]. We see that the model seems to be more accurate in reproducing the measured dose rates following the first 40 flights (8 June 2015 and onward), overestimating them by 7% on average. Also shown in Figure 4, are the average latitudinal and longitudinal positions for each flight as well as the cutoff rigidity computed by the model. Figure 5 shows that most of the significant variations in the airline dose rates are due to differences in geographic position which largely determines the cutoff rigidity.

The average dose equivalent rate measured for the flights shown in Figure 4 is 0.55 μSv/h. With an average flight time of 7.3 h, the average dose equivalent for each flight is 3.99 μSv. This means it would take approximately 1830 flight hours or 250 flights to reach the 1 mSv yearly effective dose limit for members of the public recommended by the International Commission on Radiological Protection (ICRP) and many more than that to reach the 20 mSv yearly limit for flight crew members [*ICRP*, 2007]. To provide further context, the average effective dose associated with a chest X-ray is 0.1 mSv [*Mettler et al.*, 2008], equivalent to about 25 flights. From this we can see that the radiation risks to commercial airline passengers are most likely fairly low, with relatively few airline customers flying frequently enough to approach the radiation limit recommended by

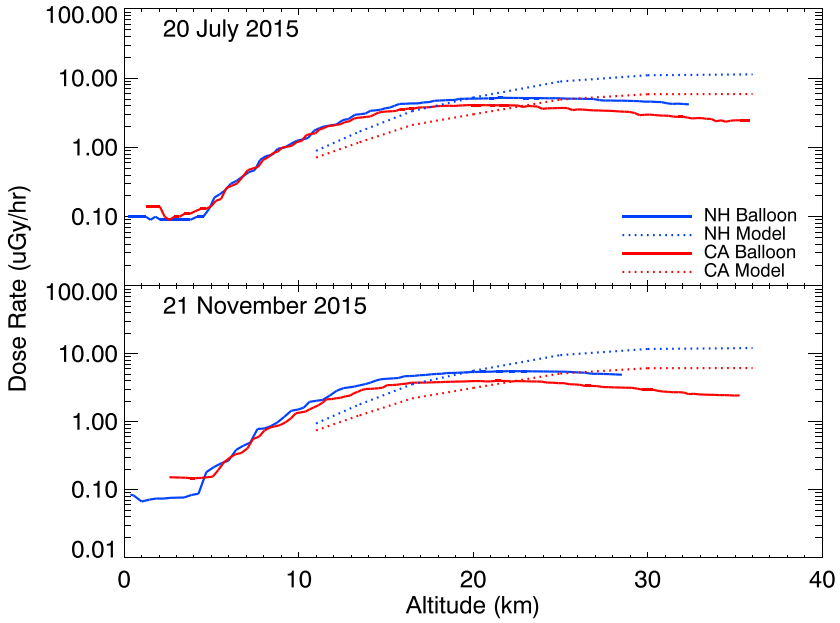

Figure 6. Dose rates measured by instruments aboard high-altitude balloons for two simultaneous launches from California and New Hampshire as well as modeled dose rates for the same times and locations.

the ICRP. As a part of its duty limitations and rest requirements, the Federal Aviation Administration (FAA) limits flight crew members to 1000 h of flight time in any 365 consecutive calendar day period (according to 14 CFR Part 117.23 of the current FAA Code of Federal Regulations), meaning that it would be unlikely for flight crew members to exceed the ICRP public dose limits under normal circumstances. The FAA does not seem to apply similar limits to other aircraft crew members such as flight attendants, so it may be possible for them to come closer to the ICRP public limit, though very unlikely to approach the much higher limit for crew members. While the current rest requirements have the secondary effect of preventing flight crew from exceeding the ICRP dose limits, specific safety requirements for limiting radiation may need to be put into place in the future with the possibility of new supersonic commercial flights flying at higher altitudes, as well as suborbital reusable launch vehicle flights to altitudes around 100 km. From Figure 3, we can see that the absorbed dose increases by more than a factor of 4 from 11 to 20 km, which is close to the maximum cruising altitude of the Concorde supersonic passenger jet (18.3 km). Assuming a similar scaling of the effective dose, it becomes more conceivable for aircraft crew members to approach the ICRP radiation limits, though rotating crew between supersonic and subsonic aircraft would likely reduce these risks significantly. SEPs events provide an additional and transient source of radiation that could potentially push crew member exposures closer to the ICRP limits. Powerful solar storms can inject energetic particles into the atmosphere, elevating radiation levels above the normal background associated with GCRs.

Measurements from the two simultaneous launches from California and New Hampshire that occurred on 20 July and 21 November 2015 are shown in Figure 6, along with the comparable modeled dose rates. We see that the model dose rates are somewhat higher than the measurements at high altitudes and somewhat lower at low altitudes, with the measured radiation levels reaching a Pfotzer maximum at approximately 20 km, while the Pfotzer maximum for the modeled dose rates exists above 36 km as previously noted. These differences are due to the fact that the balloon dosimeters measure X-rays and gamma rays rather than the primary GCRs and secondary particles used in the model. From Figure 6, we can see that particles dominate the dose rate at high altitudes, while the dose at low altitudes is dominated by photons. At high altitudes, the secondary X-rays and gamma rays are in lower abundance due to low atmospheric densities; however, following the Pfotzer maximum, they are able to penetrate deeply into the atmosphere resulting in relatively high dose rates at low altitudes. It is important to note that while the photons represent a larger portion of the total absorbed dose at airline altitudes, because particles, in particular heavy ions and neutrons, have relatively high biological damage potential as can be seen by the radiation weighting factors used to determine equivalent, gray-equivalent and effective doses [*ICRP*, 2007; *NCRP Report 132*, 2000], primary and secondary GCR

particles almost certainly represent the largest radiation threat to airline passengers. We see that the model shows a similar, though larger increase in dose rates from California to New Hampshire than the balloon measurements, with the radiation differences being due to the fact that geomagnetic cutoff rigidities are typically twice as large at California compared to New Hampshire. At 20 km, the approximate altitude where the balloon dose rates are at their highest, the measured dose rate at New Hampshire is approximately 24% higher than at California for the July launch and 36% higher for the November launch, with the changes in these percentages between launches being due to differences in the modulation potential and geomagnetic activity. Because the model uses energetic particles rather than gamma rays and X-rays, the differences in the cutoff rigidities between the two locations have a larger effect on the dose rate, resulting in much larger differences in the modeled dose rates at 20 km for both launches, with a 74% difference for July and 78% for November.

4. Conclusion

We have provided a validation of the updated model originally presented by *Joyce et al.* [2014] using ARMAS measurements made by instruments aboard 117 airline flights spanning from mid-2013 to early 2016. Improvements to the model consist of corrected dose lookup tables and the incorporation of the geomagnetic cutoff method described by *Nymmik et al.* [2009] to account for the effect of the Earth's magnetic field on atmospheric radiation levels, enabling the model to compute dose rates for any geographic position. We find the modeled radiation levels at airline altitudes to be sufficiently accurate to assess radiation risks, with the model overestimating the dose rate by 20% on average, falling within the 30% uncertainty limit recommended by the ICRU [*ICRU*, 2010]. One source contributing to the uncertainty is the transport of GCRs through the heliosphere. A series of papers in 2014 showed that different transport models can lead to differences of up to 50% in the resulting effective dose [*Slaba and Blattnig*, 2014a, 2014b; *Slaba et al.*, 2014]. We leave a detailed analysis of how these different models affect the model's output to a future study.

We have also presented a new data set of radiation measurements made by instruments aboard high-altitude balloons during 27 launches that occurred from late 2014 to early 2016 as a part of the Earth to Sky Calculus project. Because the instruments used measure gamma rays and X-rays rather than the primary and secondary GCR particles we model, they cannot be used for validation purposes; however, they do provide an interesting demonstration of the radiation profiles of photons versus particles as a function of altitude. While the comparison between the model and ARMAS measurements at airline altitudes is reassuring, a thorough validation over a range of altitudes would provide an even more useful assessment of the model. The Earth to Sky Calculus program is working to improve the measuring capabilities of its balloon payloads, including enabling the measurements of radiation due to particles such as neutrons. These additional measurements would be an invaluable contribution to the scientific community and would provide an improved capability to assess the accuracy of atmospheric radiation models.

The validation shown here lends credibility to a model that is relatively simple and relies on lookup tables rather than resource intensive computer simulations, making it easy to adapt for future efforts in risk assessment and atmospheric radiation studies. It would be relatively easy, for example, for the model to incorporate SEP flux data, such as those available on the Predictions of Radiation from Release, EMMREM, and Data Incorporating the CRaTER, COSTEP and other SEP measurements (PREDICCS) website (http://prediccs.unh.edu), to compute near real-time atmospheric dose rates due to SEP events. It also must be noted that while CRaTER provides an excellent means of computing the modulation potential, other space or ground based measurements could be used to estimate the modulation potential if CRaTER measurements were no longer available, likely with somewhat different results. We plan to make the modeled atmospheric dose rates shown here available to the community as a tool for risk assessment on the PREDICCS website, as well as the Community Coordinated Modeling Center (http://ccmc.gsfc.nasa.gov/).

Acknowledgments
Support for this work is provided by the NASA Lunar Reconnaissance Orbiter Project (NASA contract NNG11PA03C), as well as various NASA grants (EMMREM, grant NNX07AC14G; C-SWEPA, grant NNX07AC14G; DoSEN, grant NNX13AC89G; DREAM, grant NNX10AB17A; and DREAM2; grant NNX14AG13A) and an NSF grant (Sun-2-Ice, grant AGS1135432). We thank the International Space Science Institute for supporting the Research Team: Radiation Interactions at Planetary Bodies (http://www.issibern.ch/teams/interactplanetbody/). The CRaTER data used here are available on the CRaTER website: http://crater-web.sr.unh.edu/. The high-altitude balloon radiation data shown here were collected as part of the Earth to Sky Calculus program http://earthtosky.net/. The commercial airline altitude dose rates shown here were provided by the ARMAS project and are available at http://sol.spacenvironment.net/~ARMAS/Level_2_3_Data.html. Sunspot data are provided by the Solar Influences Data Analysis Center (http://www.sidc.be/silso/datafiles). The geographic map used in Figure 5 was obtained from Google Maps (www.google.com/maps/).

References

Badhwar, G. D., and P. M. O'Neill (1992), An improved model of galactic cosmic radiation for space exploration missions, *Int. J. Radiat. Appl. Instrum.*, *20*(3), 403–410, doi:10.1016/1359-0189(92)90024-P.

Chin, G., et al. (2007), Lunar Reconnaissance Orbiter overview: The instrument suite and mission, *Space Sci. Rev.*, *129*(4), 391–419.

International Commission on Radiological Protection (ICRP) (2007), ICRP publication 103, *Ann. ICRP*, *37*, 2–4.

International Commission on Radiation Units and Measurements (ICRU) (2010), Radiation protection considerations, *J. ICRU*, *10*(2), 13–15, doi:10.1093/jicru/ndq020.

Joyce, C. J., et al. (2013), Validation of PREDICCS using LRO/CRaTER observations during three major solar events in 2012, *Space Weather*, *11*, 350–360, doi:10.1002/swe.20059.

Joyce, C. J., et al. (2014), Radiation modeling in the Earth and Mars atmospheres using LRO/CRaTER with the EMMREM module, *Space Weather*, *12*, 112–119, doi:10.1002/2013SW000997.

Joyce, C. J., et al. (2015), Analysis of the potential radiation hazard of the 23 July 2012 SEP event observed by STEREO A using the EMMREM model and LRO/CRaTER, *Space Weather*, *13*, 560–567, doi:10.1002/2015SW001208.

Mettler, F. A., et al. (2008), Effective doses in radiology and diagnostic nuclear medicine: A catalog, *Radiology*, *248*, 254–263.

NASA (2007), *Space Flight Human System Standard Volume 1: Crew Health, NASA-STD-3001*, NASA, Washington, D. C.

NCRP Report 132 (2000), *Radiation Protection Guidance for Activities in Low-Earth Orbit*, Univ. of Michigan, Natl. Counc. on Radiat. Prot. and Meas., Bethesda, Md.

Nealy, J. E., F. A. Cucinotta, J. W. Wilson, F. F. Badavi, T. P. Dachev, B. T. Tomov, S. A. Walker, G. De Angelis, S. R. Blattnig, and W. Atwell (2007), Pre-engineering spaceflight validation of environmentalmodels and the 2005 HZETRN simulation code, *Adv. Space Res.*, *40*, 1593–1610, doi:10.1016/j.asr.2006.12.029.

Nymmik, R. A., M. I. Panasyuk, V. V. Petrukhin, and B. Y. Yushkov (2009), A method of calculation of vertical cutoff rigidity in the geomagnetic field, *Cosmic Res.*, *47*(3), 191–197.

O'Neill, P. M. (2006), Badhwar O'Neill galactic cosmic ray model update based on advanced composition explorer (ACE) energy spectra from 1997 to present, *Adv. Space Res.*, *37*(9), 1727–1733, doi:10.1016/j.asr.2005.02.001.

Schwadron, N. A., et al. (2010), Earth-Moon-Mars radiation environment module framework, *Space Weather*, *8*, S00E02, doi:10.1029/2009SW000523.

Schwadron, N. A., et al. (2012), Lunar radiation environment and space weathering from the Cosmic Ray Telescope for the Effects of Radiation (CRaTER), *J. Geophys. Res.*, *117*, E00H13, doi:10.1029/2011JE003978.

Schwadron, N. A., et al. (2014), Does the worsening galactic cosmic radiation environment observed by CRaTER preclude future manned deep space exploration?, *Space Weather*, *12*, 622–632, doi:10.1002/2014SW001084.

Slaba, T. C., and S. R. Blattnig (2014a), GCR environmental models I: Sensitivity analysis for GCR environments, *Space Weather*, *12*, 217–224, doi:10.1002/2013SW001025.

Slaba, T. C., and S. R. Blattnig (2014b), GCR environmental models II: Uncertainty propagation methods for GCR environments, *Space Weather*, *12*, 225–232, doi:10.1002/2013SW001026.

Slaba, T. C., X. Xu, S. R. Blattnig, and R. B. Norman (2014), GCR environmental models III: GCR model validation and propagated uncertainties in effective dose, *Space Weather*, *11*, 233–245, doi:10.1002/2013SW001027.

Spence, H. E., et al. (2010), CRaTER: The cosmic ray telescope for the effects of radiation experiment on the Lunar Reconnaissance Orbiter mission, *Space Sci. Rev.*, *150*, 243–284, doi:10.1007/s11214-009-9584-8.

Townsend, L. W., T. M. Miller, and T. A. Gabriel (2005), HETC radiation transport code development for cosmic ray shielding applications in space, *Radiat. Prot. Dosim.*, *116*(1–4), 135–139, doi:10.1093/rpd/nci091.

Townsend, L. W., M. PourArsalan, F. A. Cucinotta, M. Y. Kim, and N. A. Schwadron (2011), Transmission of galactic cosmic rays through Mars atmosphere, *Space Weather*, *9*, S00E11, doi:10.1029/2009SW000564.